

Impact of Retinal Disease-Associated RPE65 Mutations on Retinoid Isomerization[†]

Grzegorz Bereta,[‡] Philip D. Kiser,[‡] Marcin Golczak,[‡] Wenyu Sun,[‡] Elise Heon,^{§,||} David A. Saperstein,[⊥] and Krzysztof Palczewski^{*‡}

Department of Pharmacology, School of Medicine, Case Western Reserve University, Cleveland, Ohio 44106-4965, Department of Ophthalmology, University of Washington, Seattle, Washington 98195, Department of Ophthalmology and Vision Sciences, The Hospital for Sick Children, University of Toronto, Toronto, Ontario, Canada, and Program of Genetics and Genomic Biology, The Hospital for Sick Children, Toronto, Ontario, Canada M5G 1X8

Received May 14, 2008; Revised Manuscript Received June 10, 2008

ABSTRACT: Pathogenic mutations in the *RPE65* gene are associated with a spectrum of congenital blinding diseases in humans. We evaluated changes in the promoter region, coding regions, and exon/intron junctions of the *RPE65* gene by direct sequencing of DNA from 36 patients affected with Leber's congenital amaurosis (LCA), 62 with autosomal recessive retinitis pigmentosa (arRP), and 21 with autosomal dominant/recessive cone-rod dystrophies (CORD). Fifteen different variants were found, of which 6 were novel. Interesting was Gly244Val, a novel mutation close to the catalytic center. To assess the role of this mutation in RPE65 inactivation, we performed detailed biochemical studies of the mutant along with a structural analysis of the 244 amino acid position with respect to amino acids known to be important for RPE65-dependent retinoid isomerization. Bicistronic plasmid expression of the RPE65 Gly244Val mutant and enhanced green fluorescent protein (EGFP) allowed us to document both its instability in cultured cells by cell sorting and immunoblotting methodology and its loss of RPE65-dependent isomerase activity by enzymatic assays. Further insights into the structural requirements for retinoid isomerization by RPE65 were obtained by using the carotenoid oxygenase (ACO) from *Synechocystis* (PDB accession code 2BIW) as a structural template to construct a RPE65 homology model and locating all known inactivating mutations including Gly244Val within this model.

The visual (retinoid) cycle is the fundamental process responsible for production of 11-*cis*-retinal, the chromophore of rhodopsin and cone pigments (1). The importance of retinoid metabolic transformations that occur in photoreceptors and retinal pigmented epithelium (RPE)¹ is underscored by identification of retinal dystrophy-associated mutations in all genetically encoded enzymes and retinoid-binding proteins of that cycle (2). Among retinal dystrophies the most severe is Leber's congenital amaurosis (LCA), a leading cause of inherited childhood blindness. LCA is an autosomal recessive, early onset severe retinal dystrophy that accounts for 5% of all inherited retinal dystrophies (3). Of the visual cycle enzymes, mutations in RDH12 (retinol dehydrogenase 12) (4, 5), RPE65 (retinal pigmented epithelium-specific protein with molecular mass 65 kDa) (6, 7), and LRAT

(lecithin:retinol acyltransferase) (8, 9) are known to cause this type of blindness.

RPE65 is the long sought after retinoid isomerase that produces 11-*cis*-retinol from all-*trans* retinyl esters (10–12). This enzyme is a highly abundant protein in the RPE and belongs to the carotenoid oxygenase family (13, 14). Although the mechanism of isomerization is not fully understood, RPE65, like other carotenoid oxygenase family members, contains an iron cofactor essential for its activity (11). A crystal structure of one of the carotenoid oxygenase family members reveals the general architecture of this family of enzymes featuring a Fe²⁺-(His)₄ arrangement in the center of a seven-bladed β-propeller fold where the Fe²⁺ ion is accessible through a long nonpolar tunnel through which carotenoids or retinoids travel to reach the active site (15).

Mutations in RPE65 cause LCA (6) or retinitis pigmentosa (RP) (7). Since the original studies were done, a large number of individuals with retinal disease have been investigated for mutations in this gene (2). Detailed analyses of visual function in patients of different ages with mutations in RPE65 were evaluated (16, 17). In primates, the central RPE layer showed greater retinoid isomerase activity and protein levels of RPE65 compared to the more peripheral RPE (18).

Significant progress has been made in understanding the pathological basis of diseases caused by inactivating mutations in the RPE65. First, the RPE of RPE65 knockout mice was found to contain large amounts of retinyl esters that accumulated because they could not be processed further to generate 11-*cis*-retinol (19). Naturally inactivating mutations

[†] This research was supported in part by grants from the National Eye Institute (EY009339), National Institutes of Health (K.P.), Foundation Fighting Blindness (K.P.), Visual Science Training Program Grant 2T32EY007157 from the National Eye Institute (P.D.K.), and Mira Godard Research Fund (E.H.).

* Address correspondence to this author. Phone: 216-368-4631. Fax: 216-368-1300. E-mail: kxp65@case.edu.

[‡] Case Western Reserve University.

[§] University of Toronto.

^{||} The Hospital for Sick Children.

[⊥] University of Washington.

¹ Abbreviations: ACO, carotenoid oxygenase; ad, autosomal dominant; ar, autosomal recessive; CORD, cone-rod dystrophy; EGFP, enhanced green fluorescent protein; LCA, Leber's congenital amaurosis; LRAT, lecithin:retinol acyltransferase; RPE, retinal pigmented epithelium; RPE65, retinal pigmented epithelium protein with molecular mass 65 kDa; RP, retinitis pigmentosa.

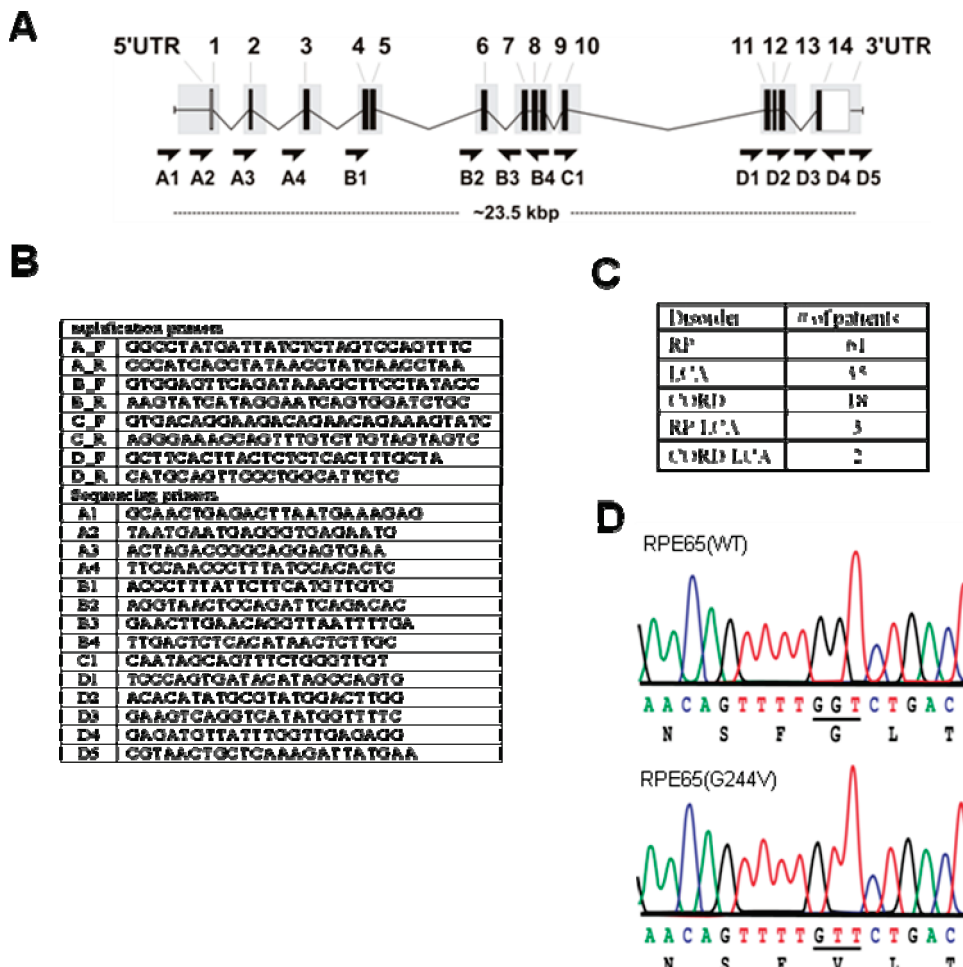


FIGURE 1: Analysis of variations in *RPE65* gene by direct sequencing of DNA from patients with retinal degeneration. (A) *RPE65* gene structure. Vertical bars represent exons and connecting lines depict introns. Arrows represent primers used for sequencing. Sequencing coverage is represented by gray rectangles. (B) Primers used for amplification (four overlapping fragments) and sequencing of the *RPE65* gene. (C) Phenotype and number of patients included in this study. (D) Sequencing chromatograms showing a fragment of the WT *RPE65* gene and the Gly244Val substitution identified for the first time in this study.

of *RPE65* in mice and dogs also were identified that caused generally poor visual function (20, 21). Moreover, partial inactivation of *RPE65* leads to a milder visual deterioration as demonstrated in mice carrying an Arg91Trp mutation that also has been identified in humans (22). Availability of LCA and RP animals led to rapid development of gene transfer and pharmacological interventions to restore vision as a prelude for treating these diseases in humans (23–26). Outcomes of the first two human gene transfer trials recently have been reported (27, 28).

Biochemical analysis of the spectrum of mutations found in a human population is important for understanding normal mechanisms of *RPE65* action and disease pathology as well as identifying patients who would most benefit from emerging therapies. To assess the role of key residues in *RPE65* function, we used direct DNA sequencing to analyze genomic DNA from 119 patients afflicted with LCA, RP, and CORD for mutations of the coding sequences, intron/exon junction regions, and promoter region of the *RPE65* gene. Fifteen different exonic variants were found, of which seven were novel. Detailed biochemical analyses of a novel Gly244Val mutation in the *RPE65* gene and structural modeling with the carotenoid oxygenase (ACO) template provided supportive information about the role of certain critical residues,

such as the Fe²⁺-coordinating His residues, in the mechanism of retinoid isomerization.

MATERIALS AND METHODS

Patient Data Collection. This study involved 119 patients with clinical diagnoses of LCA, RP, and CORD (Figure 1C). Consent and/or assent forms were obtained from all participants. Patient information and DNA samples were collected in compliance with the Health Information Portability and Accountability Act (HIPAA), policies of the Institutional Review Boards of the University of Washington, Seattle, WA, and Case Western Reserve University, Cleveland, OH, and those of the Research Ethics Board of the Hospital for Sick Children, Toronto, Canada. This project also respected the tenets of the Declaration of Helsinki.

Mutation Screening. DNA was isolated from blood samples by a standard salt precipitation technique, and the full sequence of the *RPE65* gene was amplified by PCR as four overlapping fragments by using the primer pairs listed in Figure 1A,B. Each reaction mix (50 μL) contained ~10 ng of DNA, 0.5 mM dNTP, 400 nM of each primer, 5 μL of reaction buffer (provided with polymerase), and 0.3 μL of Triple Master polymerase (Eppendorf, Hamburg, Germany). PCR cycling conditions were 93 °C for 3 min, 10 ×

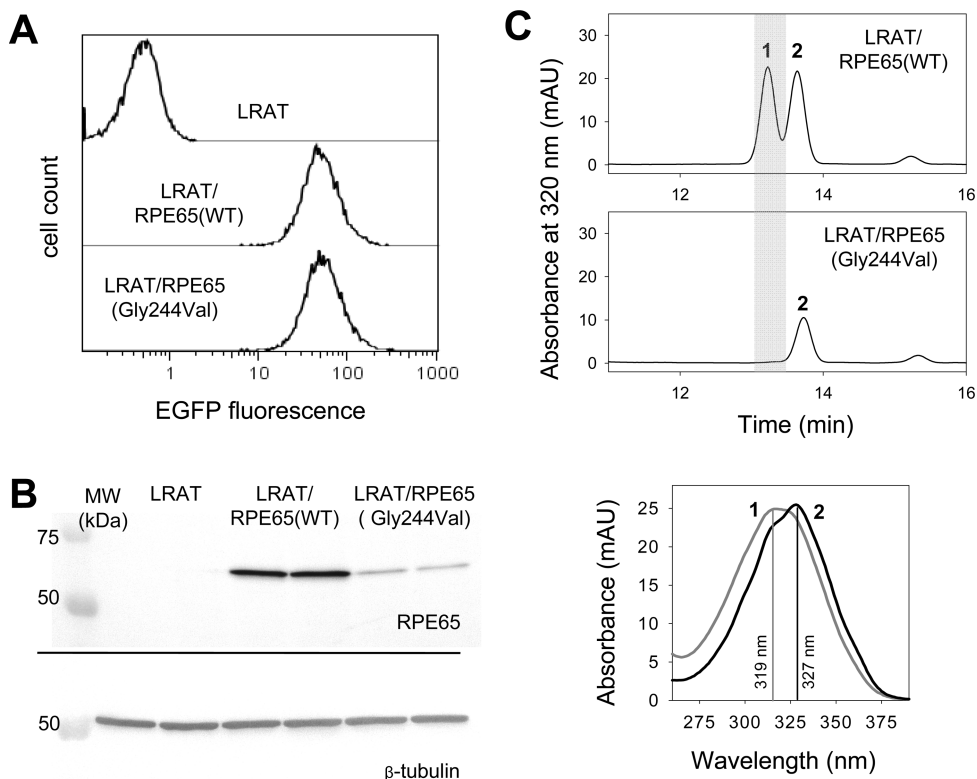


FIGURE 2: Analysis of mRNA expression and enzymatic activity of the RPE65(WT) and RPE65(Gly244Val) mutant proteins. (A) Flow cytometry analysis of EGFP fluorescence in NIH3T3 cells overexpressing LRAT, LRAT/RPE65(WT), or LRAT/RPE65(Gly244Val). The RPE65 transfer vector contains a RPE65-IRES-EGFP cassette (RPE65 and EGFP share the same mRNA) so a similar distribution of EGFP fluorescence intensity in RPE65(WT) and RPE65(Gly244Val) expressing cells indicates similar levels of RPE65 mRNA. (B) Immunoblot of RPE65(WT) and RPE65(Gly244Val) proteins expressed in NIH3T3/LRAT cells. Lower expression of RPE65(Gly244Val) mutant protein as compared to RPE65(WT) is apparent. Equal sample loading was verified by probing with β -tubulin antibody. Each sample was run in duplicate. (C) HPLC analysis of the enzymatic activity of RPE65(WT) and RPE65(Gly244Val). NIH3T3 cells overexpressing LRAT/RPE65(WT) or LRAT/RPE65(Gly244Val) were incubated with 10 μ M all-trans-retinol in growth medium for 16 h followed by organic extraction of retinoids. Enzyme activity (production of 11-cis-retinol) was monitored by normal phase HPLC. Peaks were identified based on elution time and absorbance spectra (below) that were identical with synthetic standards (1, 11-cis-retinol; 2, 13-cis-retinol). In contrast to RPE65(WT), RPE65(Gly244Val) had no enzymatic activity. mAU, milliabsorbance units.

(93 °C for 15 s, 62 °C for 30 s, and 68 °C for 8 min), and 30 \times (93 °C for 15 s, 62 °C for 30 s, and 68 °C for 8 min + 20 s/cycle). Following amplification, a 0.5 μ L aliquot of each sample was visualized on 1% agarose gel to confirm the presence of a properly sized product. The remaining sample (49.5 μ L) was incubated at 37 °C for 1 h with shrimp alkaline phosphatase (USB Corp., Cleveland, OH) and exonuclease I (USB), 5 units each, to dephosphorylate nucleotides and remove unused primers that interfere with sequencing reactions. Enzymes then were deactivated by a 15 min incubation at 80 °C. Sequencing samples were prepared by using BigDye Terminator v3.0 chemistry (Applied Biosystems, Foster City, CA) and the primers listed in Figure 1B. Sequence data were acquired with an ABI 3730 DNA analyzer and analyzed by Phred/Phrap/Consed/PolyPhred software (University of Washington, Seattle, WA). Identified novel changes were validated by assessment of nucleotide/amino acid conservation, biochemical assays, and screening of a control population of a minimum of 300 chromosomes. Segregation analysis was not possible in most cases.

Mutagenesis and Expression of RPE65. The RPE65 clone was purchased from the American Type Culture Collection (Manassas, VA) and cloned into the multicloning site (MCS) of the pMXs-IG3 retroviral vector by using EcoRI and NotI restriction sites appended to the coding sequence by PCR. The pMXs-IG3 vector was derived from a pMXs-IG vector

provided by Dr. T. Kitamura (University of Tokyo) (29) by slight modification of the MCS and adjacent sequence. The novel sequence of pMXs-IG3 is the following: [...]GAAT-TCCTGCAGGC]GGCCGCTCGAGCCCCCTCTC-CCTCCCCA[CCCCCTAACGTTACTG...], where sequences common to both vectors are shown in brackets. The RPE65 Gly244Val mutation was introduced by PCR amplification of the entire plasmid by using Phusion high-fidelity polymerase (New England Biolabs, Ipswich, MA). The fragment encompassing the RPE65-IRES-EGFP cassette, where IRES is the internal ribosome entry site (30, 31), was sequenced to ensure that only the desired mutation was introduced. NIH3T3-LRAT-RPE65 and NIH3T3-LRAT-RPE65(Gly244Val) stable cell lines were generated by transduction of the NIH3T3-LRAT stable cell line following the protocol described in ref 32. Both cell lines were sorted using a FACSaria cell sorter (BD Biosciences, San Jose, CA) to ensure similar EGFP fluorescence intensity profiles that corresponded to similar levels of RPE65 mRNA. Importantly, the vector's bicistronic design resulted in both RPE65 and the enhanced green fluorescent protein (EGFP) being expressed from a common mRNA. Just prior to performing experiments, both cell lines were reanalyzed by flow cytometry to confirm similar EGFP expression (Figure 2A).

Isomerization Activity Assay in Cell Culture. NIH3T3-LRAT, NIH3T3-LRAT-RPE65, and NIH3T3-LRAT-RPE65-

(Gly244Val) cells were seeded in six-well culture plates at 0.8×10^6 cells per well in growth medium (GM) consisting of Dulbecco's modified Eagle's medium, pH 7.2, with 4 mM L-glutamine, 4500 mg/L glucose, and 110 mg/L sodium pyruvate supplemented with 10% fetal bovine serum, 100 units/mL penicillin, and 100 units/mL streptomycin. The isomerization reaction was initiated 24 h later by exchange of GM for one containing all-trans-retinol delivered in *N,N*-dimethylformamide to a 10 μM final concentration and carried out for 16 h in a cell culture incubator (37 °C, 5% CO₂). Subsequently, the cells and medium were collected, mixed with an equal volume of 4 M KOH in methanol, and incubated at 52 °C for 2.5 h to hydrolyze retinoid esters. Next, an equal volume of hexane was added, and retinoids were extracted by vigorous shaking. Following 15 min centrifugation at 4000 rpm to facilitate phase separation, the organic phase was collected, dried down, and redissolved in 250 μL of hexane. Extracted retinoids were separated on a normal phase HPLC column (Sil; 5 μm , 4.6 \times 250 mm; Agilent Technologies, Santa Clara, CA) equilibrated with 10% ethyl acetate in hexane at an isocratic flow rate of 1.4 mL/min.

Immunoblotting of RPE65. NIH3T3/LRAT, NIH3T3/LRAT/RPE65, and NIH3T3/LRAT/RPE65(Gly244Val) cells were plated on six-well plates at 8×10^5 cells/well, grown for 24 h, and washed with PBS (154 mM NaCl, 5.6 mM Na₂HPO₄, 1 mM KH₂PO₄, pH 7.1). Next, cells were collected by scraping in PBS with 1 μM leupeptin, pelleted by centrifugation, resuspended in 200 μL of PBS with 1 μM leupeptin, sonicated for 10 s to shear the DNA, mixed with 100 μL of SDS loading buffer, incubated for 5 min at 95 °C, and separated on 10% SDS-PAGE gels (15 μL of each sample). Following transfer to Immobilon-P (Millipore, Bedford, MA) polyvinylidene fluoride (PVDF) membranes, RPE65, and β -tubulin (the control for equal sample loading) were detected by using anti-RPE65 monoclonal antibody (Novus Biologicals, Littleton, CO) diluted 1:2000 and E7 anti- β -tubulin monoclonal antibody (Developmental Studies Hybridoma Bank, contributor Dr. M. Klymkowsky) diluted 1:3000 and the ProtoBlot II AP System (Promega, Madison, WI) following the manufacturers' protocols.

Generation of the RPE65 Homology Model. Initial RPE65 homology models were generated with the Fugue (33), Phyre (34), and 3D-Jigsaw servers. All three algorithms identified the carotenoid oxygenase (ACO) from *Synechocystis* (PDB accession code 2BIW) as the most appropriate template for construction of the RPE65 homology model. In general, each of the models was similar in those regions containing His residues 180, 241, 313, and 527 which are highly conserved among all RPE65 family members, including the apocarotenoid and β -carotenoid oxygenases (11). The model produced by Fugue was selected as our starting model since it appeared to portray the seven-bladed β -propeller fold most completely. Amino acid side chains were inserted using COOT (35) and manually adjusted to optimize both the stereochemistry and interresidue contact distances. The model was then energy-minimized by using CNS (36) with harmonic restraints placed on the residues surrounding the active site Fe²⁺. Because residues 380–415 were predicted to constitute a long unstructured loop in all three homology models, this region was omitted from our final model because it was likely to be portrayed incorrectly. All figures of the

RPE65 homology model were generated by using PyMOL version 1.0 (DeLano Scientific LLC, San Francisco, CA).

RESULTS

Mutational Analysis. Exons, exon–intron junctions, and regulatory elements of the *RPE65* gene were analyzed by direct sequencing to identify the retinal dystrophy-associated sequence variations within a group of 119 unrelated patients of different ages and ethnic origins. A total of 49 sequence variants were found, of which 3 were in the 5'-regulatory region, 15 within exons, 24 within introns, and 7 in the 3'UTRs. The great majority of these alterations were single nucleotide variations (SNVs), but we also detected two duplications and one insertion (Supporting Information Table 1). Among 15 exonic variants found, 9 were predicted to cause missense substitutions, 4 silent substitutions, 1 truncation, and 1 splicing defect (Table 1). The novel exonic variants found here include Gly244Val, His182Arg, Val189Ile, Trp288Cys, Ile291Val (all missense substitutions), Ile34Ile (a silent substitution), and 1059_1060insG (an insertion). The His182Arg and Gly244Val variants were detected in homozygous form while the other novel variants were heterozygous (Table 1, Figure 1D). We expected the His182Arg variant to be disease-associated since other substitutions at this position have been previously reported to cause LCA (discussed below). The most intriguing substitution to us was the Gly244Val variant since it is located in a critical region of the RPE65 structure (discussed below). This finding led to a detailed biochemical analysis of this variant.

Impact of the Gly244Val Mutation on RPE65 Activity. Gly244 is a highly conserved residue within RPE65 sequences of a number of vertebrate species (Supporting Information Table 2). It is localized close to His241, a key residue involved in coordination of Fe²⁺ at the enzymatic active site (11). Thus, mutation of Gly244 could have a significant effect on the enzymatic activity or stability of this protein. To test this hypothesis, we generated two lines of NIH3T3 cells stably expressing LRAT and wild-type RPE65 (LRAT/RPE65WT) or LRAT and the RPE65 mutant Gly244Val (LRAT/RPE65-Gly244Val). WT and mutated RPE65 cDNAs were positioned in the retrovirus pMXs-IG3 vector upstream of the internal ribosomal entry site (IRES) and EGFP sequence (29). Thus, the protein of interest and EGFP were expressed from a common mRNA. This arrangement allowed easy visualization of the transduced cells and maximization of expression levels by sorting cells based on GFP fluorescence intensity. Moreover, to ensure equivalent mRNA levels for WT and mutated RPE65, we collected populations of cells characterized by identical fluorescence signals for both cell lines (Figure 2A).

Immunoblotting with an anti-RPE65 monoclonal antibody confirmed robust expression of WT RPE65 upon infection of NIH3T3/LRAT cells with the retrovirus. However, the Gly244Val mutant protein level was found to be greatly reduced as compared with WT protein (Figure 2B). Considering that both LRAT/RPE65(WT) and LRAT/RPE65-(Gly244Val) cell lines had similar levels of transcript for RPE65, the observed differences in protein levels clearly suggest low stability and accelerated degradation of the Gly244Val variant.

Table 1: Exonic Sequence Variants Identified in the *RPE65* Gene by This Study^a

case no.	clinical diagnosis	sequence variation	predicted effect	ref	status	no. of times sample analyzed ^b
13846	LCA	[271C>T] + [271C>T]	Arg91Trp	7, 17	pathogenic	2
29453	LCA	[271C>T] + [271C>T]	Arg91Trp	7, 17	pathogenic	2
29172	juvenile RP	[271C>T] + [=] ^c	Arg91Trp	7, 17	unknown	1
		[1059_1060insG] + [=] ^c	no protein or truncation	this study		
22216	LCA	[545A>G] + [545A>G]	His182Arg ^d	this study	unknown	2
24725	arRP	[731G>T] + [731G>T]	Gly244Val	this study	pathogenic	2
12924	LCA	[859G>T] + [859G>T]	splicing defect ^e	38	pathogenic, previously reported as Val287Phe	2
58963	ret. dystr.	[394G>A] + [=]	Ala132Thr	7, 17	pathogenic	1
1481	RP	[394G>A] + [=]	Ala132Thr	7, 17	pathogenic	1
19055	arCORD	[963T>G] + [=]	Asn321Lys ^f	17, 37, 38	unknown	1
19322	arRP	[565G>A] + [=]	Val189Ile	this study	unknown	1
54436	arCORD	[864G>T] + [=]	Trp288Cys	this study	unknown	1
1484	RP	[871A>G] + [=]	Ile291Val ^g	this study	unknown	1
		[1301C>T] + [=]	Ala434Val ^h	3, 7, 11, 37		
22015	RP	[102C>A] + [=]	Ile341Ile ⁱ	this study	unknown	1
18784	LCA	[978G>T] + [=]	Val326Val ^j	7	unknown	1
multiple patients		[1056G>A] + [=]	Glu352Glu	7	frequent variant	
13623	RP isolated	[1155G>A] + [=]	Thr385Thr ^k	7	unknown	1

^a Nomenclature follows recommendations of the Human Genome Variation Society (www.genomic.unimelb.edu.au/mgi/mutnomen/). [=] denotes heterozygosity. ^b In cases where a homozygous pathogenic mutation was found, DNA analysis (amplification and sequencing) was repeated to confirm the result. ^c Cloning and sequencing is required to determine if these variants affect same or different alleles. ^d Substitutions of residue 182 have been reported previously but not by Arg (3, 7, 37, 47, 48). ^e Substitution c.859G>T most likely results in a splicing defect rather than a Val287Phe missense substitution as reported earlier (38). This is because Gly in position 859 is the first nucleotide of an exon and therefore an element of the splice acceptor consensus ((39); reviewed in ref 40). ^f Pathogenicity uncertain (17). ^g A sequence alignment between different species reveals that Val at position 291 is present in mice and rats, indicating that this substitution might be a rare nonpathogenic variant. ^h Interpreted as nonpathogenic because segregation analysis showed that the index case with this change was a heterozygote whereas an unaffected sibling was a homozygote (7). ⁱ The silent substitution Ile341Ile is reported here for the first time. This variant, as well as Val326Val and Thr385Thr, has never been reported in a healthy control population, i.e., 96 individuals (7) or 210 unrelated individuals from the HapMap database (all ethnicities combined). Hence, the possibility of an association with retinal dystrophy cannot be excluded. Perhaps these variants could abolish RPE65 expression by altering exonic splicing enhancers and disrupting mRNA splicing (reviewed in refs 49 and 40).

To test whether mutation of Gly244 leads to alteration of RPE65 isomerase activity, we incubated LRAT/RPE65-(Gly244Val) cells overnight with 10 μM all-trans-retinol. Analysis of retinoids extracted from the cells revealed the absence of 11-cis-retinol, indicating a complete lack of enzymatic activity (Figure 2C). The parallel experiment with WT RPE65 resulted in a robust 11-cis-retinol production of 500 pmol per 1 × 10⁶ of LRAT/RPE65(WT) cells (Figure 2C). Because the protein level of the Gly244Val mutant was significantly reduced as compared with WT, we scaled up the mutant isomerase reaction ten times but still could not detect 11-cis-retinol production (data not shown). Thus, substitution at position 244 completely abolished the enzymatic activity of RPE65 under conditions where the mutant mRNA was fully expressed.

Homology Modeling of RPE65. Availability of a crystal structure of a carotenoid oxygenase family member, *Synechocystis* ACO (15), allowed us to build a three-dimensional model of RPE65 to explore for possible mechanisms by which the pathogenic mutations identified in this (Table 1) and other studies (Supporting Information Table 2) might disrupt protein function. The accuracy of our model depends on the homology between RPE65 and ACO. Regions of the protein where homology is higher (e.g., the catalytic center and its vicinity) could be modeled more accurately than regions of low homology such as loops and helices at the protein exterior. His182 and Gly244 were found in close proximity to the conserved Fe²⁺-binding His residues of the catalytic core (Figure 3A,B). Therefore, substitutions at these positions should cause displacement of Fe²⁺-binding His residues, resulting in a decreased affinity of RPE65 for Fe²⁺ and a decrease in this protein's enzymatic activity and/or stability. Our biochemical studies of the Gly244Val variant

as well as reports regarding substitutions of His182 (11) agree with this hypothesis.

DISCUSSION

Characterization of Sequence Variants Found in the RPE65 Gene. In this study, sequence analysis of the *RPE65* gene (encoding the retinoid isomerohydrolase of the visual cycle) revealed multiple sequence variants throughout the gene (Supporting Information Table 1). We restricted our focus to variants detected in exons (Table 1) since the disease relevance of variants within other sequences (introns, regulatory regions) would be more difficult to establish.

The novel variants, Gly244Val and His182Arg, were homozygous and appeared especially intriguing because these substitutions are located near the Fe²⁺-chelating core and adjoin each other in the model RPE65 structure (Figure 3A,B) based on homology to carotenoid oxygenase (Materials and Methods). Furthermore, both substitutions are also positioned close to the Fe²⁺-chelating His residues; His182 is separated by a single amino acid and Gly244 by two amino acids from His180 and His241, respectively. These observations suggest that substitutions of Gly244 and His182 by other residues could displace the Fe²⁺-chelating His residue causing loss of Fe²⁺ from the active site with ensuing loss of enzymatic activity and possibly structural stability as well. This concept is supported by the nature of the Gly residue, because it lacks a side chain and therefore can adopt a wide range of conformations due to minimal steric hindrance. Replacement of Gly with a Val residue could thus prevent the Fe²⁺-chelating center from adopting the correct conformation. Here we did show with the Gly244Val RPE65 mutant expressed in a heterologous system that the Gly244Val

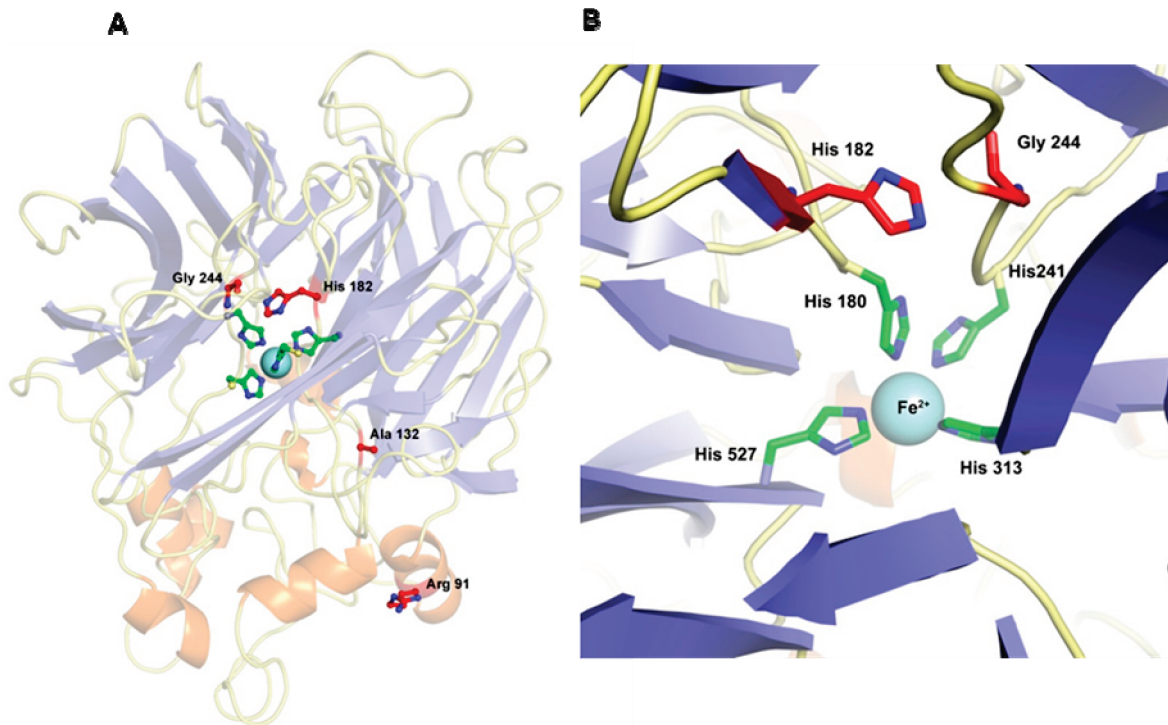


FIGURE 3: RPE65 homology model showing positions of pathogenically mutated residues found in this study. Residues 200–235 are omitted in the figure for clarity. The red colored carbon atoms of the side chains indicate pathogenically mutated amino acids, and the green colored ones indicate His residues coordinating Fe^{2+} . The Fe^{2+} ion is represented as a teal sphere. (A) Residues found in our study, substitutions of which are associated with retinal dystrophy. (B) A close-up view of residues His182 and Gly244 showing their proximity to the catalytic core, specifically His180 and His241, which suggests that these mutations may disrupt Fe^{2+} coordination and consequently affect the enzyme's stability and/or activity.

substitution caused destabilization of the protein, resulting in accelerated degradation and complete lack of activity. This demonstrated that Gly244 has an important structural role in the RPE65 protein, which is in agreement with the hypothesis that Fe^{2+} binding might be affected. To investigate this hypothesis further, analysis of Fe^{2+} -binding to the mutant protein is warranted. This presents a formidable challenge because the mutant protein is readily degraded and fails to accumulate within the cell. Interestingly, the patient carrying the Gly244Val variant of RPE65 retained residual vision in his third decade of life (Supporting Information Figure 1 and Table 3), indicating that the mutant protein, in contrast to the cell culture experiment, retains some activity. This seeming disparity implies that there might be factors specific to the retina, such as RPE65-binding proteins, which increase stability and/or activity of the mutant protein. Similarly, the Arg91Trp variant overexpressed in a heterologous system was reportedly inactive (49), but retained residual activity when expressed in mouse retina (25).

As for the His182 residue, even though the Arg substitution has never been reported, other substitutions at this position, His182Tyr (7, 37) and His182Asn (3), have been shown to be associated with LCA. Furthermore, the stability and/or activity of those variants were impaired as demonstrated by biochemical studies (11). These findings confirm the importance of having the proper residue in position 182 and suggest that the His182Arg mutant is likely to be unstable and associated with disease as well. On the other hand, ACO, an enzyme related to RPE65, has an Arg at a corresponding position, indicating that the Arg substitution could have a milder effect than those by Tyr or Asn.

The homozygous substitution c.859G>T found in an LCA patient most likely results in a splicing defect rather than a Val287Phe missense substitution as reported earlier (38). This is because Gly in position 859 is the first nucleotide of an exon and therefore an element of the splice acceptor consensus ((39); reviewed in ref 40). Such a splicing defect is predicted to eliminate RPE65 expression and production of 11-cis-retinal, resulting in a more severe visual phenotype compared to cases where amino acid substitutions decrease but do not eliminate RPE65 activity. This agrees with clinical data (Supporting Information Table 3) showing that the patient carrying the c.859G>T variant has a severe dystrophy.

The Arg91Trp variant that has been commonly reported in many previous studies (7, 17, 37, 38, 41, 42) is probably the most common disease-associated alteration in the *RPE65* gene. In this study also, the Arg91Trp substitution was the most prevalent disease-associated variant, being detected in three instances, twice in homozygous and once in heterozygous form (Table 1). A biochemical evaluation of the Arg91Trp variant was carried out using a cell line expressing the mutant protein (43) and more recently by characterizing RPE65 Arg91Trp knock-in mice (22). Both reports agree that the stability and levels of this RPE mutant protein are greatly reduced. However, residual isomerase activity was found in knock-in mouse retina while it was undetectable in cells overexpressing this mutant protein. This disparity could result from lower sensitivity of the cell based assay or the lack of retina specific factors affecting the activity and/or proper membrane localization (mislocalization had been proposed in cell culture study) of the mutant RPE65. Our homology model shows that Arg91 is located in an α -helical

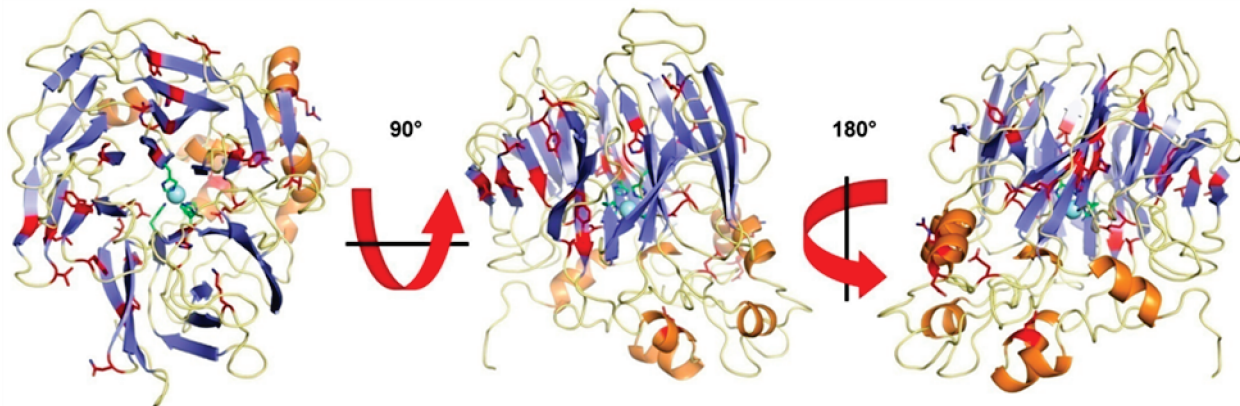


FIGURE 4: Location of all pathogenically mutated residues reported to date within the RPE65 structure. Residues affected in retinal dystrophy (colored red) are located throughout many regions of this protein and therefore are predicted to exert their deleterious effects by several different mechanisms. Some mutations seem to cluster, stressing the importance of the affected regions for the protein's activity and/or stability (discussed below).

region at the exterior of the protein (Figure 3A), and thus, exchange of a positively charged Arg residue for an aromatic, uncharged Trp residue could destabilize local structure and accelerate degradation of this enzyme.

The Ala132Thr variant has been reported in RP patients in homozygous (7) and heterozygous forms (17), and the disease relevance of this variant was supported by segregation analysis (7). Surprisingly, biochemical studies indicated that this variant retained 50% of WT activity (44) and might provide enough 11-cis-retinal to maintain a healthy retina. To resolve this discrepancy, more comprehensive patient data and a better understanding of RPE65 function are required. We found the Ala132Thr variant in heterozygous form in two patients. Our inability to find a sequence alteration in the other allele could have resulted from incomplete sequencing coverage of the *RPE65* gene or another gene might have caused the clinical disorder. In our model of the RPE65 structure, the Ala132 residue is hidden inside the molecule but not close to the catalytic center (Figure 3A). Since the amino acid sequence in the vicinity of Ala132 is not conserved between the RPE65 and ACO proteins, our homology model of the protein may not be accurate in this region so we can only speculate as to the molecular effect(s) of the Ala132Thr substitution.

We colored all affected residues in the RPE65 homology model red (Figure 4) to determine whether the disease-associated RPE65 variants reported to date are localized to discrete regions of the protein or are distributed randomly. This revealed that the mutations are located in many regions of the protein. Thus, they could exert deleterious effects in many different ways, e.g., by impairing Fe^{2+} binding or substrate channeling, disrupting the local or global structure, or affecting binding of putative protein partners. Interestingly, some residues altered in retinal dystrophy seem to be clustered rather than distributed randomly. An especially obvious example is the location of Arg44, His68, Tyr79, and Gly528 residues within a single β -sheet (Figure 5). Substitution of any of these residues could destabilize this β -sheet and displace the Fe^{2+} -chelating His527 located on its innermost strand. This in turn could affect Fe^{2+} binding and cause a reduction in RPE65 enzymatic activity. Similarly, residues Thr457, Leu450, Tyr435, and Glu436 are also found within a single β -sheet (Figure 6). Substitutions of these residues may affect the positioning of Glu417 predicted to

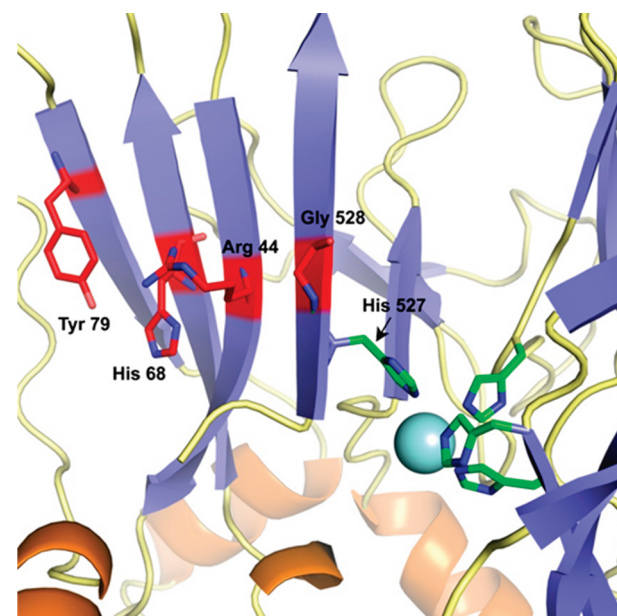


FIGURE 5: An example of clustering of pathogenically mutated residues in human RPE65. Residues 416–523 are omitted from the model for clarity. Substitutions of residues Arg44, His68, Tyr79, and Gly528 (colored red) were identified as a cause of retinal dystrophy. These residues are located in a single β -sheet, suggesting a common disease mechanism that destabilizes the β -sheet. This in turn might result in displacement of the Fe^{2+} -chelating His527, impaired Fe^{2+} binding, and a consequent reduction in RPE65 enzymatic activity.

form an ion–dipole interaction with His313 (Figure 6). Loss of this interaction could alter the Lewis base properties of His313 and reduce its metal binding capability. Regarding the aforementioned Leu450 residue, its naturally occurring Met substitutions are frequently found in laboratory mice where they affect the rate of chromophore regeneration (see below).

Effect of the Leu450Met Mutation on RPE65 Structure and Enzymatic Activity. In addition to human mutations in RPE65, spontaneously occurring variants in RPE65 have been identified in other species that contribute to our understanding of this protein's role in ocular physiology. One such example is that a greatly improved resistance to light-induced retinal damage in C57Bl/6 mice was directly associated with a hypomorphic variant of mouse RPE65 (45).

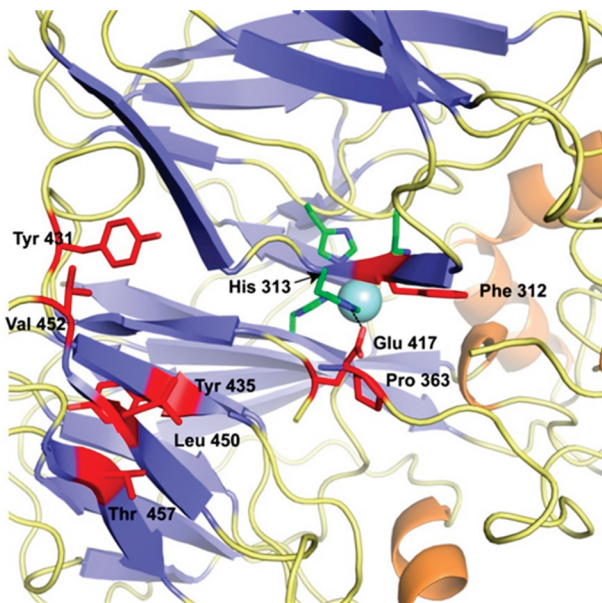


FIGURE 6: A hypothetical mechanism by which Leu450 substitutions might affect the RPE65 enzymatic activity. Residues 365–379 and 323–331 are omitted from the model for clarity. Leu450 is located in a β -sheet close to other residues known to be pathogenically mutated (colored red). This encourages us to propose a possible mechanism by which its substitutions might affect RPE65 activity. Mutations in this region could disrupt the β -sheet fold and affect positioning of Glu417 which is predicted to form an ion–dipole interaction with His313 (shown as a dashed black line). Loss of this interaction could alter the Lewis acid properties of His313 and reduce its metal binding capacity. The well-known Leu450Met substitution found in mice, which reduces but does not eliminate isomerase activity, may only slightly perturb this region due to the relative similarities between the Leu residue and Met side chains. In contrast, the Leu450Arg substitution found in retinal dystrophy patients introduces a positive charge into this region so it is likely to disrupt the fold to a greater extent.

Light damage susceptibility was proportional to the rate of rhodopsin regeneration, which determines rhodopsin availability during light exposure. Light damage found in two strains with Leu450 in RPE65 was correlated with the occurrence of photoreceptor apoptosis after short bright light exposure. In contrast, mice with the Leu450Met variation regenerated rhodopsin more slowly and evidenced increased resistance to light-induced retinal degeneration (46). The mechanism of retinal protection can be explained by the fact that a change of a single amino acid residue (Leu450Met) in mouse RPE65 causes both lower protein expression and lower overall activity of this enzyme. Consequently, the rate of rhodopsin regeneration and its subsequent activation is reduced (44). The importance of amino acid 450 is reinforced by the greatly diminished activity and severe ocular phenotype of humans carrying the Leu450Arg mutation (50). Based on homology models to ACO, the effect of the Met450 variant on RPE65 activity was proposed to relate to the ability of the Met side chain to form hydrogen bonds with other residues in blade 6 of the protein. So this mutation might affect the secondary structure of the β -strand, flexibility of the blade, and overall stability and enzymatic activity of the protein (44). Analysis of our RPE65 model does not challenge this hypothesis. But we do note that the Glu417 residue that seems to stabilize the Fe^{2+} -chelating His residue through an ion–dipole interaction lies just at the edge of the affected β -sheet (Figure 6). This residue might be

displaced as a result of changes within that β -sheet, thereby impairing Fe^{2+} coordination. On the other hand, Leu450 is located at the periphery of RPE65 some distance from the active site of the protein. Thus, an alternative explanation for the reduced enzymatic activity of the Leu450Met variant might be a reduced ability to interact with proteins such as LRAT, RDH5, or others involved in the isomerization process. Interestingly, although Leu450 is highly conserved within RPE65 sequences of different species, effects of the Leu450 mutation on enzymatic activity may vary. *In vitro* studies show that the impact of the Leu450Met substitution is more severe in murine RPE65 as compared to the canine protein. Such differences might indicate additional, species-specific variations in surrounding residues that play important roles in modulating RPE65 activity, as was proposed for residue 446 (44).

CONCLUSIONS

Mutations in the *RPE65* gene can cause severe retinal dystrophies. Here we report 15 exonic sequence variants of *RPE65* gene, 7 of which are novel and might be associated with retinal dystrophies. The novel RPE65 Gly244Val mutation was characterized in biochemical detail. We introduced bicistronic plasmid expression of this mutant together with EGFP enabling tight control and monitoring of the mRNA level, which permitted precise evaluation of this mutant's stability and activity in cell culture experiments. Molecular modeling of RPE65 provided important information as to how several mutations might impact retinoid isomerization by RPE65 and lead to photoreceptor degeneration.

ACKNOWLEDGMENT

We thank Yesmino Elia for coordinating patient scheduling and Alex Levin for contributing to patient recruitment. We also thank Dr. T. Kitamura (University of Tokyo) for the generous gift of pMXs-IG and pMXs-IP vectors and Dr. Leslie Webster, Jr., for help during manuscript preparation.

SUPPORTING INFORMATION AVAILABLE

Table 1, genetic variation identified in the RPE65 gene in this study in patients with retinal degeneration (frequency data included); Table 2, sequence variation in the RPE65 gene and sequence alignments among the *RPE65* genes from different species; Table 3, clinical characteristics of patients with RPE65 mutations; Figure 1, retinal imaging of patient carrying the Gly244Val mutation. This material is available free of charge via the Internet at <http://pubs.acs.org>.

REFERENCES

1. Palczewski, K. (2006) G protein-coupled receptor rhodopsin. *Annu. Rev. Biochem.* 75, 743–767.
2. Travis, G. H., Golczak, M., Moise, A. R., and Palczewski, K. (2007) Diseases caused by defects in the visual cycle: retinoids as potential therapeutic agents. *Annu. Rev. Pharmacol. Toxicol.* 47, 469–512.
3. Hanein, S., Perrault, I., Gerber, S., Tangy, G., Barbet, F., Ducrocq, D., Calvas, P., Dollfus, H., Hamel, C., Lopponen, T., Munier, F., Santos, L., Shalev, S., Zafeiriou, D., Dufier, J. L., Munnich, A., Rozet, J. M., and Kaplan, J. (2004) Leber congenital amaurosis: comprehensive survey of the genetic heterogeneity, refinement of the clinical definition, and genotype-phenotype correlations as a strategy for molecular diagnosis. *Hum. Mutat.* 23, 306–317.
4. Janecke, A. R., Thompson, D. A., Utermann, G., Becker, C., Hubner, C. A., Schmid, E., McHenry, C. L., Nair, A. R.,

- Ruschendorf, F., Heckenlively, J., Wissinger, B., Nurnberg, P., and Gal, A. (2004) Mutations in RDH12 encoding a photoreceptor cell retinol dehydrogenase cause childhood-onset severe retinal dystrophy. *Nat. Genet.* 36, 850–854.
5. Perrault, I., Hanein, S., Gerber, S., Barbet, F., Ducrocq, D., Dollfus, H., Hamel, C., Dufier, J. L., Munnich, A., Kaplan, J., and Rozet, J. M. (2004) Retinal dehydrogenase 12 (RDH12) mutations in leber congenital amaurosis. *Am. J. Hum. Genet.* 75, 639–646.
6. Gu, S. M., Thompson, D. A., Srikanthi, C. R., Lorenz, B., Finckh, U., Nicoletti, A., Murthy, K. R., Rathmann, M., Kumaramanickavel, G., Denton, M. J., and Gal, A. (1997) Mutations in RPE65 cause autosomal recessive childhood-onset severe retinal dystrophy. *Nat. Genet.* 17, 194–197.
7. Morimura, H., Fishman, G. A., Grover, S. A., Fulton, A. B., Berson, E. L., and Dryja, T. P. (1998) Mutations in the RPE65 gene in patients with autosomal recessive retinitis pigmentosa or leber congenital amaurosis. *Proc. Natl. Acad. Sci. U.S.A.* 95, 3088–3093.
8. Thompson, D. A., Li, Y., McHenry, C. L., Carlson, T. J., Ding, X., Sieving, P. A., Apfelstedt-Sylla, E., and Gal, A. (2001) Mutations in the gene encoding lecithin retinol acyltransferase are associated with early-onset severe retinal dystrophy. *Nat. Genet.* 28, 123–124.
9. Senechal, A., Humbert, G., Surget, M. O., Bazalgette, C., Bazalgette, C., Arnaud, B., Arndt, C., Laurent, E., Brabet, P., and Hamel, C. P. (2006) Screening genes of the retinoid metabolism: novel LRAT mutation in leber congenital amaurosis. *Am. J. Ophthalmol.* 142, 702–704.
10. Moiseyev, G., Chen, Y., Takahashi, Y., Wu, B. X., and Ma, J. X. (2005) RPE65 is the isomeroxydrolase in the retinoid visual cycle. *Proc. Natl. Acad. Sci. U.S.A.* 102, 12413–12418.
11. Redmond, T. M., Poliakov, E., Yu, S., Tsai, J. Y., Lu, Z., and Gentleman, S. (2005) Mutation of key residues of RPE65 abolishes its enzymatic role as isomeroxydrolase in the visual cycle. *Proc. Natl. Acad. Sci. U.S.A.* 102, 13658–13663.
12. Jin, M., Li, S., Moghrabi, W. N., Sun, H., and Travis, G. H. (2005) Rpe65 is the retinoid isomerase in bovine retinal pigment epithelium. *Cell* 122, 449–459.
13. Schwartz, S. H., Tan, B. C., Gage, D. A., Zeevaart, J. A., and McCarty, D. R. (1997) Specific oxidative cleavage of carotenoids by VP14 of maize. *Science* 276, 1872–1874.
14. von Lintig, J., and Wyss, A. (2001) Molecular analysis of vitamin A formation: cloning and characterization of beta-carotene 15,15'-dioxygenases. *Arch. Biochem. Biophys.* 385, 47–52.
15. Kloer, D. P., Ruch, S., Al-Babili, S., Beyer, P., and Schulz, G. E. (2005) The structure of a retinal-forming carotenoid oxygenase. *Science* 308, 267–269.
16. Jacobson, S. G., Cideciyan, A. V., Aleman, T. S., Sumaroka, A., Schwartz, S. B., Windsor, E. A., Roman, A. J., Heon, E., Stone, E. M., and Thompson, D. A. (2007) RDH12 and RPE65, visual cycle genes causing leber congenital amaurosis, differ in disease expression. *Invest. Ophthalmol. Visual Sci.* 48, 332–338.
17. Thompson, D. A., Gyurus, P., Fleischer, L. L., Bingham, E. L., McHenry, C. L., Apfelstedt-Sylla, E., Zrenner, E., Lorenz, B., Richards, J. E., Jacobson, S. G., Sieving, P. A., and Gal, A. (2000) Genetics and phenotypes of RPE65 mutations in inherited retinal degeneration. *Invest. Ophthalmol. Visual Sci.* 41, 4293–4299.
18. Jacobson, S. G., Aleman, T. S., Cideciyan, A. V., Heon, E., Golczak, M., Beltran, W. A., Sumaroka, A., Schwartz, S. B., Roman, A. J., Windsor, E. A., Wilson, J. M., Aguirre, G. D., Stone, E. M., and Palczewski, K. (2007) Human cone photoreceptor dependence on RPE65 isomerase. *Proc. Natl. Acad. Sci. U.S.A.* 104, 15123–15128.
19. Redmond, T. M., Yu, S., Lee, E., Bok, D., Hamasaki, D., Chen, N., Goletz, P., Ma, J. X., Crouch, R. K., and Pfeifer, K. (1998) Rpe65 is necessary for production of 11-cis-vitamin A in the retinal visual cycle. *Nat. Genet.* 20, 344–351.
20. Pang, J. J., Chang, B., Hawes, N. L., Hurd, R. E., Davisson, M. T., Li, J., Noorwez, S. M., Malhotra, R., McDowell, J. H., Kaushal, S., Hauswirth, W. W., Nusinowitz, S., Thompson, D. A., and Heckenlively, J. R. (2005) Retinal degeneration 12 (rd12): a new, spontaneously arising mouse model for human Leber congenital amaurosis (LCA). *Mol. Vision* 11, 152–162.
21. Aguirre, G. D., Baldwin, V., Pearce-Kelling, S., Narfstrom, K., Ray, K., and Acland, G. M. (1998) Congenital stationary night blindness in the dog: common mutation in the RPE65 gene indicates founder effect. *Mol. Vision* 4, 23.
22. Samardzija, M., von Lintig, J., Tanimoto, N., Oberhauser, V., Thiersch, M., Reme, C. E., Seeliger, M., Grimm, C., and Wenzel, A. (2008) R91W mutation in Rpe65 leads to milder early-onset retinal dystrophy due to the generation of low levels of 11-cis-retinal. *Hum. Mol. Genet.* 17, 281–292.
23. Acland, G. M., Aguirre, G. D., Ray, J., Zhang, Q., Aleman, T. S., Cideciyan, A. V., Pearce-Kelling, S. E., Anand, V., Zeng, Y., Maguire, A. M., Jacobson, S. G., Hauswirth, W. W., and Bennett, J. (2001) Gene therapy restores vision in a canine model of childhood blindness. *Nat. Genet.* 28, 92–95.
24. Acland, G. M., Aguirre, G. D., Bennett, J., Aleman, T. S., Cideciyan, A. V., Bennicelli, J., Dejneka, N. S., Pearce-Kelling, S. E., Maguire, A. M., Palczewski, K., Hauswirth, W. W., and Jacobson, S. G. (2005) Long-term restoration of rod and cone vision by single dose rAAV-mediated gene transfer to the retina in a canine model of childhood blindness. *Mol. Ther.* 12, 1072–1082.
25. Van Hooser, J. P., Aleman, T. S., He, Y. G., Cideciyan, A. V., Kuksa, V., Pittler, S. J., Stone, E. M., Jacobson, S. G., and Palczewski, K. (2000) Rapid restoration of visual pigment and function with oral retinoid in a mouse model of childhood blindness. *Proc. Natl. Acad. Sci. U.S.A.* 97, 8623–8628.
26. Van Hooser, J. P., Liang, Y., Maeda, T., Kuksa, V., Jang, G. F., He, Y. G., Rieke, F., Fong, H. K., Detwiler, P. B., and Palczewski, K. (2002) Recovery of visual functions in a mouse model of Leber congenital amaurosis. *J. Biol. Chem.* 277, 19173–19182.
27. Maguire, A. M., Simonelli, F., Pierce, E. A., Pugh, E. N., Jr., Mingozi, F., Bennicelli, J., Banfi, S., Marshall, K. A., Testa, F., Surace, E. M., Rossi, S., Lyubarsky, A., Arruda, V. R., Konkle, B., Stone, E., Sun, J., Jacobs, J., Dell'Osso, L., Hertle, R., Ma, J. X., Redmond, T. M., Zhu, X., Hauck, B., Zelenai, O., Shindler, K. S., Maguire, M. G., Wright, J. F., Volpe, N. J., McDonnell, J. W., Auricchio, A., High, K. A., and Bennett, J. (2008) Safety and efficacy of gene transfer for Leber's congenital amaurosis. *N. Engl. J. Med.* 358, 2240–2248.
28. Bainbridge, J. W., Smith, A. J., Barker, S. S., Robbie, S., Henderson, R., Balaggan, K., Viswanathan, A., Holder, G. E., Stockman, A., Tyler, N., Petersen-Jones, S., Bhattacharya, S. S., Thrasher, A. J., Fitzke, F. W., Carter, B. J., Rubin, G. S., Moore, A. T., and Ali, R. R. (2008) Effect of gene therapy on visual function in Leber's congenital amaurosis. *N. Engl. J. Med.* 358, 2231–2239.
29. Kitamura, T., Koshino, Y., Shibata, F., Oki, T., Nakajima, H., Nosaka, T., and Kumagai, H. (2003) Retrovirus-mediated gene transfer and expression cloning: powerful tools in functional genomics. *Exp. Hematol.* 31, 1007–1014.
30. Liu, X., Constantinescu, S. N., Sun, Y., Bogen, J. S., Hirsch, D., Weinberg, R. A., and Lodish, H. F. (2000) Generation of mammalian cells stably expressing multiple genes at predetermined levels. *Anal. Biochem.* 280, 20–28.
31. Mancia, F., Patel, S. D., Rajala, M. W., Scherer, P. E., Nemes, A., Schieren, I., Hendrickson, W. A., and Shapiro, L. (2004) Optimization of protein production in mammalian cells with a coexpressed fluorescent marker. *Structure* 12, 1355–1360.
32. Golczak, M., Maeda, A., Bereta, G., Maeda, T., Kiser, P. D., Hunzelmann, S., von Lintig, J., Blaner, W. S., and Palczewski, K. (2008) Metabolic basis of visual cycle inhibition by retinoid and nonretinoid compounds in the vertebrate retina. *J. Biol. Chem.* 283, 9543–9554.
33. Shi, J., Blundell, T. L., and Mizuguchi, K. (2001) FUGUE: sequence-structure homology recognition using environment-specific substitution tables and structure-dependent gap penalties. *J. Mol. Biol.* 310, 243–257.
34. Bennett-Lovsey, R. M., Herbert, A. D., Sternberg, M. J., and Kelley, L. A. (2008) Exploring the extremes of sequence/structure space with ensemble fold recognition in the program Phyre. *Proteins* 70, 611–625.
35. Emsley, P., and Cowtan, K. (2004) Coot: model-building tools for molecular graphics. *Acta Crystallogr.* 60, 2126–2132.
36. Brunger, A. T., Adams, P. D., Clore, G. M., DeLano, W. L., Gros, P., Grosse-Kunstleve, R. W., Jiang, J. S., Kuszewski, J., Nilges, M., Pannu, N. S., Read, R. J., Rice, L. M., Simonson, T., and Warren, G. L. (1998) Crystallography & NMR system: A new software suite for macromolecular structure determination. *Acta Crystallogr.* 54, 905–921.
37. Simovich, M. J., Miller, B., Ezzeldin, H., Kirkland, B. T., McLeod, G., Fulmer, C., Nathans, J., Jacobson, S. G., and Pittler, S. J. (2001) Four novel mutations in the RPE65 gene in patients with Leber congenital amaurosis. *Hum. Mutat.* 18, 164.
38. Lotery, A. J., Namperumalsamy, P., Jacobson, S. G., Weleber, R. G., Fishman, G. A., Musarella, M. A., Hoyt, C. S., Heon, E., Levin, A., Jan, J., Lam, B., Carr, R. E., Franklin, A., Radha, S., Andorf, J. L., Sheffield, V. C., and Stone, E. M. (2000) Mutation

- analysis of 3 genes in patients with Leber congenital amaurosis. *Arch. Ophthalmol.* 118, 538–543.
39. Mount, S. M. (1982) A catalogue of splice junction sequences. *Nucleic Acids Res.* 10, 459–472.
40. Wang, Z., and Burge, C. B. (2008) Splicing regulation: from a parts list of regulatory elements to an integrated splicing code. *RNA (New York)* 14, 802–813.
41. Lorenz, B., Gyurus, P., Preising, M., Bremser, D., Gu, S., Andrassi, M., Gerth, C., and Gal, A. (2000) Early-onset severe rod-cone dystrophy in young children with RPE65 mutations. *Invest. Ophthalmol. Visual Sci.* 41, 2735–2742.
42. El Matri, L., Ambresin, A., Schorderet, D. F., Kawasaki, A., Seeliger, M. W., Wenzel, A., Arsenijevic, Y., Borrut, F. X., and Munier, F. L. (2006) Phenotype of three consanguineous Tunisian families with early-onset retinal degeneration caused by an R91W homozygous mutation in the RPE65 gene. *Graefe's Arch. Clin. Exp. Ophthalmol.* 244, 1104–1112.
43. Takahashi, Y., Chen, Y., Moiseyev, G., and Ma, J. X. (2006) Two point mutations of RPE65 from patients with retinal dystrophies decrease the stability of RPE65 protein and abolish its isomero-hydrolase activity. *J. Biol. Chem.* 281, 21820–21826.
44. Redmond, T. M., Weber, C. H., Poliakov, E., Yu, S., and Gentleman, S. (2007) Effect of Leu/Met variation at residue 450 on isomerase activity and protein expression of RPE65 and its modulation by variation at other residues. *Mol. Vision* 13, 1813–1821.
45. Danciger, M., Matthes, M. T., Yasamura, D., Akhmedov, N. B., Rickabaugh, T., Gentleman, S., Redmond, T. M., La Vail, M. M., and Farber, D. B. (2000) A QTL on distal chromosome 3 that influences the severity of light-induced damage to mouse photoreceptors. *Mamm. Genome* 11, 422–427.
46. Wenzel, A., Reme, C. E., Williams, T. P., Hafezi, F., and Grimm, C. (2001) The Rpe65 Leu450Met variation increases retinal resistance against light-induced degeneration by slowing rhodopsin regeneration. *J. Neurosci.* 21, 53–58.
47. Galvin, J. A., Fishman, G. A., Stone, E. M., and Koenekoop, R. K. (2005) Evaluation of genotype-phenotype associations in leber congenital amaurosis. *Retina (Philadelphia)* 25, 919–929.
48. Galvin, J. A., Fishman, G. A., Stone, E. M., and Koenekoop, R. K. (2005) Clinical phenotypes in carriers of Leber congenital amaurosis mutations. *Ophthalmology* 112, 349–356.
49. Wang, G. S., and Cooper, T. A. (2007) Splicing in disease: disruption of the splicing code and the decoding machinery. *Nat. Rev. Genet.* 8, 749–761.
50. Wada, Y., Nakazawa, M., Abe, T., Fuse, N., and Tamai, M. (2000) Clinical variability also is found in patients with mutations in genes encoding other visual cycle proteins, e.g., arrestin, RPE65 and RDH5. *Invest. Ophthalmol. Visual Sci.* 41, S617.

BI800905V